Journal of Hydrology 599 (2021) 126291

Contents lists available at ScienceDirect

Journal of Hydrology

journal homepage: www.elsevier.com/locate/jhydrol

Research papers

Evaluating the impacts of drought on rice productivity over Cambodia in the Lower Mekong Basin

Abhijeet Abhishek [a], Narendra N. Das [d,b,a], Amor V.M. Ines [c,d], Konstantinos M. Andreadis [e], Susantha Jayasinghe [f], Stephanie Granger [b], Walter L. Ellenburg [g], Rishiraj Dutta [f], Nguyen Hanh Quyen [f], Amanda M. Markert [g], Vikalp Mishra [g], Mantha S. Phanikumar [a,*]

[a] Department of Civil and Environmental Engineering, Michigan State University, East Lansing, MI 48824, USA
[b] Jet Propulsion Laboratory, California Institute of Technology, Pasadena, CA 91109, USA
[c] Department of Plant, Soil and Microbial Sciences, Michigan State University, East Lansing, MI 48824, USA
[d] Department of Biosystems and Agricultural Engineering, Michigan State University, East Lansing, MI 48824, USA
[e] Department of Civil and Environmental Engineering, University of Massachusetts Amherst, Amherst, MA 01002, USA
[f] Asian Disaster Preparedness Center, Bangkok 10400, Thailand
[g] Earth System Science Center, The University of Alabama in Huntsville, Huntsville, AL 35805, USA

ARTICLE INFO

This manuscript was handled by Emmanouil Anagnostou, Editor-in-Chief, with the assistance of Xiaodong Zhang, Associate Editor

Keywords:
Drought
Lower Mekong Basin
Cambodia
Hydrologic modeling
Rice yield
Crop model

ABSTRACT

Recurring drought in the Lower Mekong countries has inflicted enormous pressure on the natural ecosystem, rice productivity, and water resources. A regional scale assessment over Cambodia was carried out to examine the linkages between rice productivity and meteorological/hydrologic drought variability from 2000 to 2016. We implemented a comprehensive drought and crop yield information system, the Regional Hydrologic Extremes Assessment System (RHEAS) framework, that couples a hydrologic model with a crop growth model to capture the subtle, intrinsic nature of drought, and assess the impact on inter-seasonal and intra-annual rice yields. Simulations based on RHEAS show good agreement with observations ($R^2 \sim 0.65$ for soil moisture from the hydrologic model; $R^2 \sim 0.84$ for crop model). Using a suite of standardized drought indices, the onset and prevalence of dry and wet periods throughout the study period were examined at multiple temporal scales. The temporal variability in drought intensity exhibited higher water stress during the initial months (Mar-May), indicating prevalence of medium to severe dry conditions prior to the planting season. However, the onset of monsoon at the beginning of the growing season (June) resulted in the prevalence of normal to moderate wet conditions. A linear trend analysis for the period 2000–2016 showed a consistent increase (~2900 kg/ha in 2000 to ~ 3550 kg/ha in 2016) in rice yields, although drought-stricken provinces showed lower yields (~1650 kg/ha) throughout the study period. Overall, a continuous increase in annual rice yields irrespective of the stress conditions was noted with no clear pattern linking drought parameters with crop yields on a regional scale. The application of chemical-based fertilizers has steadily increased over the years since 2008 and the consistent increase in observed rice yields correlated with increased fertilizer use ($R^2 \sim 0.84$). Information from the hydrologic and crop model components within RHEAS enables development of critical regional and local thresholds, reflecting the increasing levels of risk and vulnerability towards drought.

1. Introduction

Among all the natural hazards, drought is by far the most expensive, complex, and uncertain weather-related disaster worldwide, resulting in large annual socio-economic losses (Pandey et al., 2007). Often characterized by a prolonged deficit of precipitation and long periods of abnormally dry conditions, there is no universally accepted definition of drought (Van Loon et al., 2016a). Droughts originate from a range of hydrometeorological processes that reflect the long-term imbalance between water supply and water demand. Due to their high variability, both spatially and temporally, the effects of drought can be localized, thus making its characterization complex and uncertain. Recurring droughts have crippled countries throughout the course of human history, having profound impacts on agriculture, food security, water

* Corresponding author.
E-mail address: phani@egr.msu.edu (M.S. Phanikumar).

https://doi.org/10.1016/j.jhydrol.2021.126291
Received 23 December 2020; Received in revised form 1 March 2021; Accepted 5 April 2021
Available online 8 April 2021

resources, human livelihood, and the natural ecosystem (Wilhite, 2000). Numerous studies have attributed the severity, duration, location, and timing of droughts to regional and global scale processes: in the United States (Andreadis et al., 2005; Zhang et al., 2017), India (Aadhar and Mishra, 2017), Amazon (Duffy et al., 2015; Wongchuig Correa et al., 2017), Europe (Grillakis, 2019), Africa (Gebremeskel Haile et al., 2019; Sheffield et al., 2014), China (Zhang and Jia, 2013; Zhang et al., 2016) and have well documented the variability and the nature of drought. From these studies, it is obvious that the frequency and intensity of droughts have arguably increased over the years and exacerbated due to other adversely influencing factors (Dai, 2013; Van Loon et al., 2016b) such as population growth, rapid urbanization, land-use changes, and altering precipitation regimes. These factors, along with the impacts of climate change, have inflicted enormous pressure on many countries, thus raising serious concerns pertaining to food and water security (Godfray et al., 2010).

The over-reliance on water resources attributed to agriculture has heavily weighed on the water budget (Mishra and Singh, 2010). Diminishing natural resources, shrinking croplands, frequent exposure to extreme events (drought, floods, etc.), expansion of agricultural systems and energy/power sectors have further aggravated the situation, ultimately resulting in seasonal water shortages (Thilakarathne and Sridhar, 2017). Such changes are distinctly evident in the southern stretches of the Mekong Basin, wherein the Mekong countries have been vulnerable to the negative consequences of climate change, thus posing risks for agricultural systems and human livelihoods. The Mekong River is imperative to the region, both environmentally and economically (MRC, 2014). However, the recent infrastructure (e.g., hydropower) and irrigation developments in the upstream Mekong have changed the magnitude and seasonality of flow (Hoang et al., 2019; Pokhrel et al., 2018), especially in the lower stretches of the basin (near Tonle Sap Lake, Cambodia). In addition, extreme drought events in the past decades, notably in 1997–98, 2003–05 (IPCC, 2007) and late 2015–2016 (Guo et al., 2017; Son et al., 2012) had significant impact on the agricultural sector, leading to huge crop losses and lower agricultural productivity. Despite the increased vulnerability of agriculture to droughts, the impacts have been somewhat overlooked, and arguably less understood compared to floods (Kim et al., 2019).

Nearly 70 percent of the population is actively engaged in agricultural activities in the Lower Mekong Basin (LMB) region. Most of the agricultural systems in the region are rain-fed, thus making them vulnerable to the risks (and uncertainties) associated with seasonality (Johnston et al., 2012; MRC, 2003). As there are no alternative sources of income other than agriculture, the crop losses associated with seasonality take a huge toll on the livelihoods of the lower income and other marginalized groups (MRC, 2014). Rice, being the principal crop, is particularly sensitive to climate, and has been negatively impacted by climatic change (Mainuddin et al., 2013). The low-lying areas (near Tonle Sap Lake) and the deltaic regions of Vietnam are highly vulnerable to these physical shocks. With the increasing demand for rice production reaching an expected estimate of 3720 kg/ha and 6530 kg/ha respectively for Cambodia and Vietnam by 2025 (MRC, 2014), there is an acute need of minimizing the risks associated with seasonal extremities, and simultaneously improving the agricultural yields. There is increasing recognition of the need for both a regional and a national perspective on drought risk management interventions, to reduce the vulnerability of affected communities (ADB, 2009). Hence, there is a compelling need to monitor current hydrologic conditions, drought status, and crop yield estimates and make those data available to stakeholders on a regular basis. This information pertaining to inter-seasonal/intra-annual hydrologic, drought, and rice yield indicators and forecasts will facilitate risk management and planning for decision makers.

Despite the advent of numerous drought monitoring tools, such as the United States Drought Monitor (Svoboda et al., 2002), and the Global Drought Early Warning Monitoring Framework (GDEWF: Pozzi et al., 2013), the accurate assessment and prediction of drought characteristics still proves challenging. Inconsistent records and poor quality of spatial coverage data from ground-based observational networks has long been a primary reason hindering long-term hydro-agricultural studies. However, recent advances in dynamic modeling and the use of satellite-based observations have created the potential for operational drought monitoring (Klisch and Atzberger, 2016). The introduction of targeted drought indicators in modeling frameworks has not only improved the existing monitoring techniques (and capabilities) but facilitated insightful information on early warning, preventive measures, and mitigation strategies. Hence, using a suite of single/multivariate remote sensing-based indices (or data), the numerical representation of drought characteristics from a range of extensive hydroclimatic conditions provides useful information on the overall qualitative state of drought (Hao et al., 2015).

Oftentimes, there exists a gap between science applications and end-users, resulting in the partial implementation of effective adaptation strategies (Andreadis et al., 2017). This fundamental disconnect is distinct within the agriculture sector, so bridging the gap will be helpful in facilitating better decision making. Though many software frameworks have explored the integration of modeling systems, the internal representation of datasets has always proven to be challenging, often resulting in compatibility issues within the constituent models (Beran and Piasecki, 2009). A novel aspect of this study involves the application of the recently developed end-to-end information system Regional Hydrologic Extremes Assessment System (RHEAS: Andreadis et al., 2017), that couples physically-based hydrologic and crop models, and uses data assimilation (primarily using remote sensing observations) and projections to provide nowcasts and seasonal forecasts (3–6 months in advance) of yield estimates and associated drought indicators. While the previous study did not include any model validation, region-specific information, etc., this study incorporates site-specific information and sufficient validation against observations for effective drought and yield nowcasting. Another novel aspect of this work is the investigation of the potential impact of growing season drought states on rice yields. This information is especially important for local governments/stakeholders for facilitating decision-making. Here, we integrate readily available observations of meteorological (e.g., precipitation) and hydrologic variables (e.g., soil moisture) via a coupled hydro-agricultural model offered by the RHEAS framework to identify changes in drought conditions and their impact on rice production in the Lower Mekong region. Despite the availability of the RHEAS implementation over the entire LMB, we opted to focus our analysis on Cambodia, as its economy is especially reliant on agriculture and droughts adversely affect both livelihoods and food security. Our primary objective in this study was to assess the spatiotemporal evolution of drought and rice yields over Cambodia and to investigate the potential impacts of drought on inter-annual variability of rice yields. Using a suite of hydrologic datasets, we analyzed the derived model simulations (e.g., soil moisture, yield, etc.) with remote sensing products and other observations. The approach and results described here are expected to improve our understanding of the environmental conditions and hydrology related to crop yields by providing a quantitative historical perspective to support and improve decision-making processes.

2. Materials and methods

2.1. Study area

Located in Southeast Asia, the transboundary Mekong river has an estimated length of 4,350 km with a mean annual discharge of approximately 475 km^3, making it the tenth largest river in the world in terms of mean annual flow at its mouth (Liu et al., 2007). Depending on the location of the river, the landscape and climate range from hilly mountainous terrains (~4500 m elevation) of Lao to the low-level deltaic plains of Vietnam. Rising from high mountain ranges, the river flows through deep, narrow gorges, traverses through floodplains (for

2600 km) before entering the South China sea via a wide delta, draining an area of 810,000 km^2 (MRC, 2014; Lauri et al., 2014). The Mekong river basin is typically portioned into the "upper basin", and the "lower basin". The LMB covers about 77% (606,000 km^2) of the basin and is important both environmentally and economically. The LMB consisting of the four riparian countries– Cambodia, Lao PDR, Thailand, and Viet Nam covers an approximate area of 618,783 km^2 (Fig. 1). The region has a typical monsoon climate, having two distinct seasons- i) wet Southwest monsoon (May-Oct), and ii) dry Northeast monsoon (Nov-Apr), with annual precipitation between 1200 and 2500 mm/year respectively. The region receives ~ 85% of the annual precipitation in the wet season with the dry season bearing minimal precipitation (Kite, 2001). Temperature and evaporation rates throughout the basin vary with elevation, typically ranging between 22 and 28 ℃ and 1,000–2,000 mm/year respectively. The river flows through extensive wetland habitats supporting productive ecosystems, particularly the Tonle Sap Lake in Cambodia. The lake and its surrounding floodplains in the heart of Cambodia play an important role in inducing a seasonal change in the direction of the flow in the river. This seasonality greatly influences the floodplains and the agricultural productivity downstream (lower provinces of Cambodia) and the Mekong delta. The Tonle Sap floodplains and the delta host a population of 35 million, and account for more than 90 percent of paddy plantation (MRC, 2014). As shown in Fig. 1b, the majority of the agricultural activities and wetland ecosystems in Cambodia are concentrated along the Tonle Sap Lake and the southeastern provinces. Although substantial improvements have been made within the agriculture sector, large discrepancies in mechanization, irrigation capacity, etc. have limited the production capacity of Cambodia behind its neighboring countries (Mainuddin et al., 2013).

2.2. Model description

RHEAS was developed at the Jet Propulsion Laboratory (NASA/JPL) and has been implemented at the NASA-SERVIR hubs at the Regional Centre for Mapping of Resources for Development (RCMRD) in Nairobi and Asian Disaster Preparedness Center (ADPC) in Bangkok and covers regions over East Africa and the Lower Mekong region at a spatial resolution of 25 km (and 5 km over a limited coverage area) for different water resources applications (Andreadis et al., 2017). RHEAS integrates multiple remote sensing products across different components of the terrestrial water cycle to effectively monitor water stress as indicated by the drought status. The main component of the RHEAS architecture hosts a spatially enabled relational (PostGIS) database that ingests a suite of earth science products (model datasets and satellite observations) that provide a range of hydrologic and agricultural variables. PostGIS, an extension to PostgreSQL database, uses and extends the SQL language (combined with other features) and allows the functionality of querying and managing spatial geometries. RHEAS follows a hybrid approach that allows the seamless coupling of the constituent models, thus making its design distinct and unique from other information systems. Such design of combining modular and object-oriented programming has several advantages- i) better transferability of data across models; ii) system modularity, since all the models incorporated within the framework must interface with the PostGIS database and not the internal formats of other models. In addition, this arrangement allows easy implementation and customization with minimal input requirements from end-users, thus extending the system's applicability. Fig. 2 presents a simplified flow chart of the RHEAS architecture with the constituent models and meteorological forcing. The logic of integrating the hydrologic and crop models is intended to capture the whole gamut of hydrological processes and the full extent of process dynamics

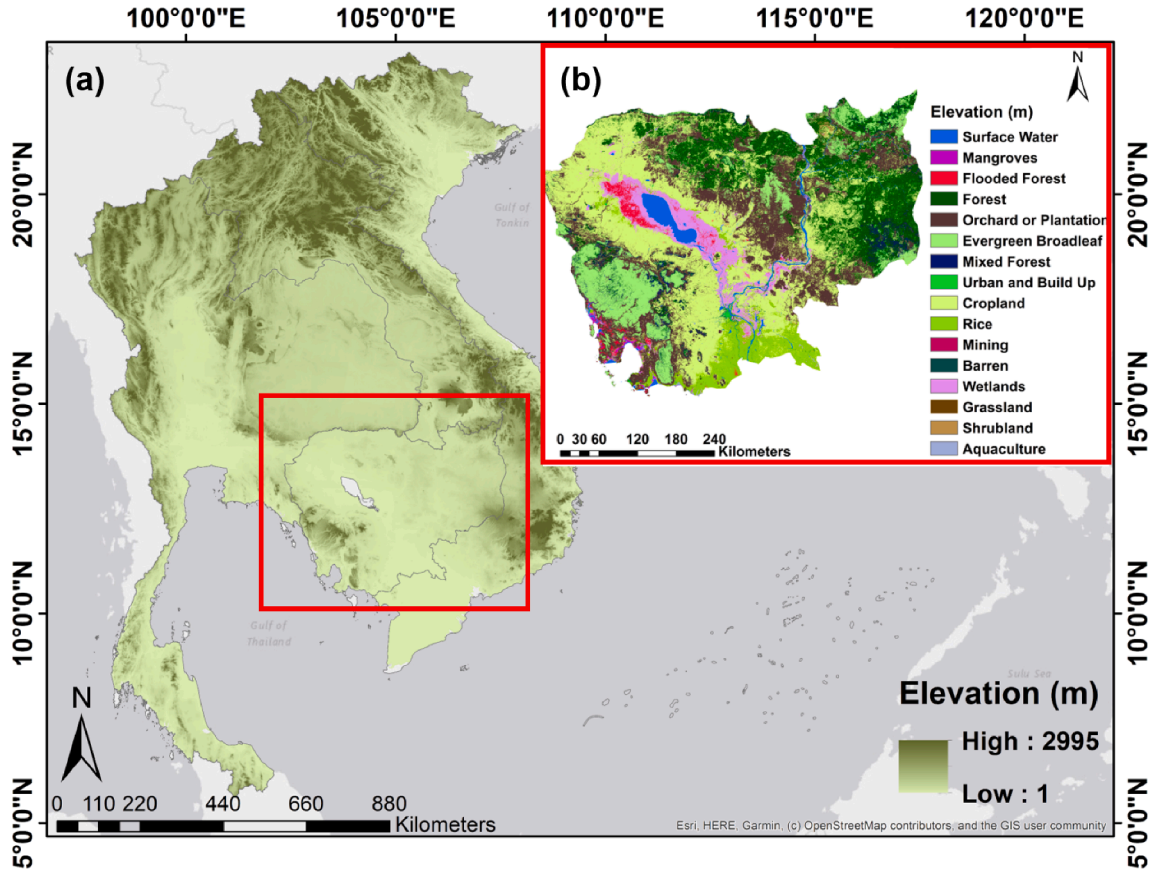

Fig. 1. (a) Map showing the Lower Mekong Basin (LMB) countries with Cambodia highlighted; (b, inset) Regional land cover/land use map of the study area Cambodia.

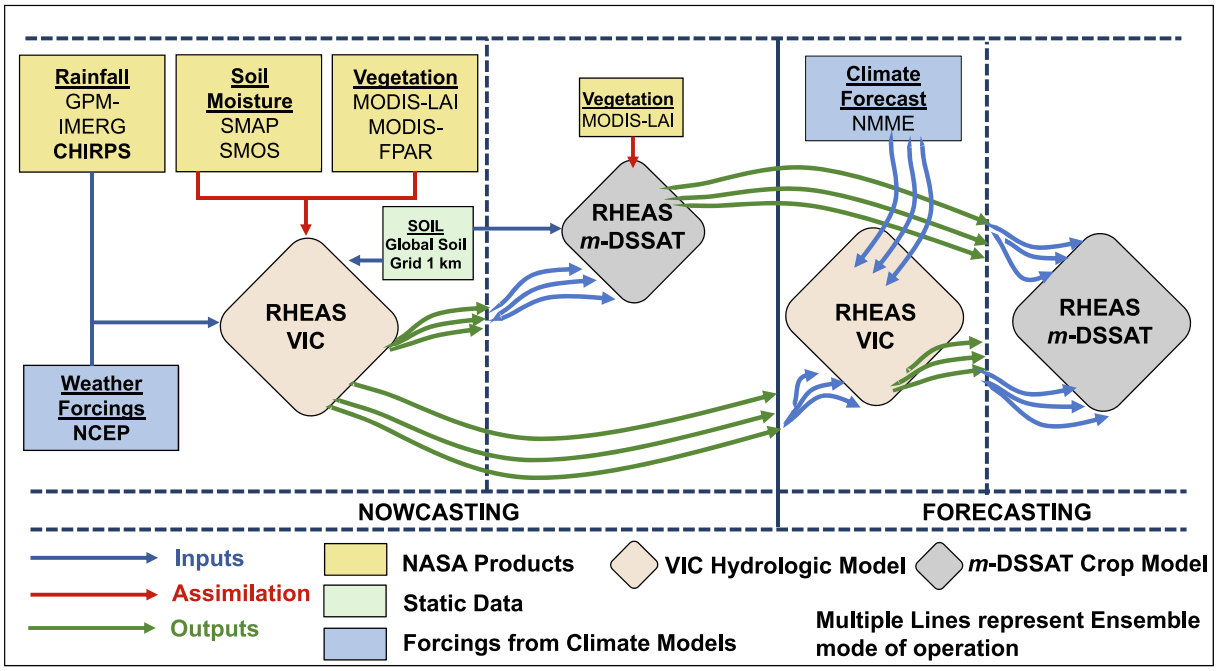

Fig. 2. Simplified flow chart of the RHEAS algorithm: RHEAS assimilates multiple remote sensing observations to provide different hydroclimatic states and drought indicators. VIC: Variable Infiltration Capacity hydrologic model; *m*-DSSAT: modified Decision Support System for Agrotechnology Transfer crop model; CHIRPS: Climate Hazards Group Infrared Precipitation with Station data; NCEP: National Centre for Environmental Prediction; SMAP: Soil Moisture Active Passive; NMME: North American Multi-Model Ensemble. Nowcasting is the present agri-hydrologic states based on past, historic records, while the forecast simulations require a model ensemble to predict the drought characteristics and crop yields at lead times of one to three months.

involved in the soil–plant-atmosphere continuum. Detailed information about the model design, architecture, installation, and operation is readily available at https://github.com/nasa/RHEAS.

The macroscale Variable Infiltration Capacity (VIC: Liang et al., 1994) hydrologic model is the primary component in the RHEAS information system. VIC simulates the land–atmosphere fluxes and computes the energy (and water) balance at the land surface at daily timesteps. In addition, VIC generates a multitude of hydrologic variables and drought indicators that are used to quantify the uncertainties across different components of the hydrologic cycle. These variables and indicators are tightly constrained by in situ and satellite observations of soil moisture, precipitation, runoff, evapotranspiration (ET), groundwater, and snow (if needed). The process-based Decision Support System for Agrotechnology Transfer (DSSAT: Jones et al., 2003) crop model is incorporated within RHEAS to simulate the crop growth, development, and yield under different management practices and soil properties. The crop component within RHEAS has a modified version of the baseline DSSAT (*m*-DSSAT) crop model with 50 ensemble members, that can stop and restart every day, whereas crop models generally run continuously from sowing until maturity/harvest (Ines et al., 2013). This modification was necessary to facilitate data assimilation of leaf area index (LAI) and soil moisture during different phases of crop growth. In addition, this refinement also helps to better capture the history of crop growth towards the harvest season by producing a realistic crop yield forecast than what could otherwise be obtained by just using model-based forcing from a seasonal climate forecast.

2.3. Data

At a minimum, all land surface models require high-quality meteorological forcings (e.g., precipitation, air temperature, and wind speed) and land cover/type information (e.g., soil properties, land cover, elevation) (Mizukami et al., 2014). The high-resolution (0.05°), near-real-time daily, and pentad Climate Hazards Group Infrared Precipitation with Station data (CHIRPS: Funk et al., 2015) gridded precipitation product was used to force the hydrologic model from 1981 through the present. Due to its long historical records, low latency, and temporally consistent datasets, the CHIRPS precipitation product was used to simulate the near-real-time initial hydrologic conditions. Many precursory studies have successfully used the CHIRPS precipitation product for flood and drought monitoring (Katsanos et al., 2016; Toté et al., 2015). Other variables, such as air temperature and wind speed, were obtained using the National Centre for Environmental Prediction (NCEP: Kalnay et al., 1996) gridded reanalysis product. The land coverage information was obtained from the Moderate Resolution Imaging Spectroradiometer (MODIS-500 m) global product at yearly intervals (Friedl et al., 2010). Information on soil characteristics is an essential component of crop model simulations. Absence of any well-established soil database and gridded products over the Mekong region has made modeling soil processes difficult (Arrouays et al., 2014). Because of the gridded nature of RHEAS, a 10 km spatial resolution soil database based on the SoilGrids1km (Han et al., 2019), was used for regional crop modeling in this study. Other ancillary information, such as fertilizer application rates and cultivar varieties were obtained from various external sources (e.g., local bodies, government agencies, etc.) and previous studies. Table 1 briefly summarizes a list of datasets that are available within the RHEAS database.

2.4. Methodology

A regional study was carried out over the LMB region, with an extensive focus over Cambodia for the period of 1981–2019. The simulations were performed by providing information on the mode of operation (nowcast/forecast), selection of simulation type (crop: *m*-DSSAT/hydrologic: VIC) through a text-based configuration file. After the ingestion of the required forcing (and ancillary information), the VIC hydrologic model explicitly computes the hydrologic and drought characteristics for each grid cell (0.25°) over the study region. VIC has a unique representation of sub-grid variability and better characterization of vertical soil moisture distribution, thus making it an ideal choice for

Table 1
Datasets available within the RHEAS database.

Parameter	Product	Spatial Resolution	Temporal Resolution	Temporal Coverage
Precipitation	GPM IMERG	10 km	Daily	2014 – present
	TMPA	25 km	Daily	1998 – present
	CMORPH	8 km	Daily	1998 – present
	CHIRPS*	5 km	Daily	1981 – present
	PERSIANN-CDR	25 km	Daily	1983 – present
Temperature*	NCEP	1.875 deg	Daily	1948 – present
Wind Speed*	NCEP	1.875 deg	Daily	1948 – present
Soil Moisture**	SMAP	~9 km	2–3 days	2015 – present
	SMOS	40 km	2–3 days	2010 – present
SAR Backscatter¶	Sentinel 1A/B	<1km	12 days	2016 – present
Evapotranspiration**	MOD16	1 km	8 days	2000 – present
Leaf Area Index**	MOD15	1 km	8 days	2002 – present
Seasonal Climate* Forecast	NMME	2.5	Monthly	2000 – present

Note: *: forcings **: data assimilation ¶: ancillary data for planting information.

hydrologic simulations. Another important aspect of VIC is calibration of the model parameters for hydrologic applications. However, we have opted to not perform additional calibrations on top of the VIC model calibrations previously reported in the literature for two reasons. Firstly, as RHEAS is a modeling framework aimed at deployments in data-poor regions, our objective was to evaluate its performance with as little in-situ data as possible. Moreover, the default parameters included in the RHEAS implementation were derived from a global calibration of the VIC model performed in several previous studies (Sheffield and Wood, 2007; Zhang et al., 2018) that demonstrated the accuracy of the model when simulating hydrologic fluxes and states.

In this study, we have solely focused on agricultural and meteorological droughts. Agricultural drought is especially intricate and difficult to distinguish from other types due to the high disparity of water requirement for different crops. RHEAS uses the Soil Moisture Deficit Index (SMDI) and Drought Severity indicator for characterizing agricultural drought. The SMDI computes weekly soil water deficit to represent the overall soil water availability in the root zone. Using the long-term median of weekly averaged soil water, and maximum and minimum weekly soil water recording, SMDI provides the soil moisture deficit (in percent) at various depths of the soil profile. This information is especially used to discern the optimal crop water requirements of different crops at various stages of growth. Likewise, the drought severity index allows for the categorization of various levels of moisture availability (dryness/wetness), wherein the moisture content is expressed as a percentile of the model climatology for each grid cell. Precipitation is the most critical variable that is subjected to major fluctuations compared to other hydrologic states such as runoff, soil moisture, groundwater. Thus, quantifying the impact of precipitation deficit on other hydrologic states (e.g., streamflow, groundwater) will help characterize meteorological drought. Hence, the normalized SPI was used to reflect the precipitation deficit at multiple timescales (notably 1-, 3-, 6- and 12-month). Based on the historic long-term precipitation records, the SPI provides a standardized value for dry/wet conditions for a specific period. Tables S1 and S2 (Supplementary Material) provide information on SPI and SMDI on a standardized scale where positive values represent wet and negative values represent dry conditions. Also, RHEAS generates other indicators such as Standardized Runoff Index (SRI) and Dryspells, which are used to characterize hydrologic drought conditions. Information regarding the frequency of drought (dry spells, i.e., number of days between two drought events) supplements the system and plays a vital role in decision making during the growing season.

Following a similar technique as mentioned above, the crop model simulations were carried out by providing the essential information through a configuration file. Using the same information and model forcings (same as VIC), the modified DSSAT (*m*-DSSAT) model is run on a yearly basis to generate the inter-annual yields. It becomes extremely important to supplement the crop model with specific information on local practices (such as rice cultivar types in the region, planting dates from crop calendar) for optimal modeling of agricultural productivity. Typical information on management practices was obtained from local bodies, governments, and previous studies. Although no specific information on cultivar varieties and fertilizer application rates were available from local authorities in Cambodia, we used the information from previous studies and World Bank/FAO (Food and Agriculture Organization). For rice cultivar genetic coefficients, calibration using in situ field data is essential under no stress condition (Boote, 1999). The calibrated cultivar should achieve the observed yield and biomass. Since we did not have any field data of rice cultivation under no stress condition, we adapted the calibrated rice cultivars (genetic coefficients) for Cambodia from Wang et al., 2017 who used field data under no stress condition. The rice cultivar genetic coefficients from Wang et al., 2017 (Table S3, Supplementary Material) are well calibrated with the field experiment conducted in 2011 and validated against yield data from years 2010 and 2013. Wang et al., 2017 reported that the simulated yields of rice cultivars were nearly same as the observed yields in the calibration year 2011, while 1.2 to 3.1% of rice yields were higher in the validation years 2010 and 2013, respectively.

The VIC-generated outputs are used to initialize the surface boundary conditions and root-zone profiles of the crop model, i.e., *m*-DSSAT through an Ensemble Kalman Filter (EnKF) (Evensen, 2003). Fig. 3 illustrates the integration of classical sequential EnKF (Houtekamer and Mitchell., 1998; Whitaker and Hamill, 2002) within the DSSAT-CSM. In this approach, the *m*-DSSAT runs 50 ensemble members simultaneously, while waiting to subsequently update the next suite of state variables and model parameters when observations or measured data are available. The EnKF assimilation is done when observations are available to update the model forecasts to generate the analysis, which caters as input for the next timestep of ensemble DSSAT modeling. The ensembles are run through DSSAT model again until the next update of observations are available. These model ensembles are used to estimate the uncertainties in crop modeling simulations by capturing the structural and internal variability in agricultural systems, arising from either model parameter values, fertilizer rates, soil profile, or other ancillary information. In this framework, input and output (I/O) variables and the updated variables from EnKF are stored in software modules and then passed as arguments to the crop model to re-initialize/restore the current model variable values before the model proceeds with integration to the next time step. The RHEAS framework performs data assimilation of surface soil moisture (Das and Mohanty, 2006, Das et al., 2008) and LAI (Ines et al., 2013). The data assimilation of surface soil moisture also updates the status of root-zone soil moisture. This is accomplished by using the covariance matrix of the soil profile. Unlike the assimilation of surface soil moisture, the assimilation of LAI (from MODIS data) is not straightforward. This is because LAI is physically related to many other vegetation-related variables and parameters e.g., plant leaf area, leaf weight, and plant carbohydrates. The values of updated LAI from data assimilation are used to adjust these variables for each ensemble member before simulating the next time step of the crop model.

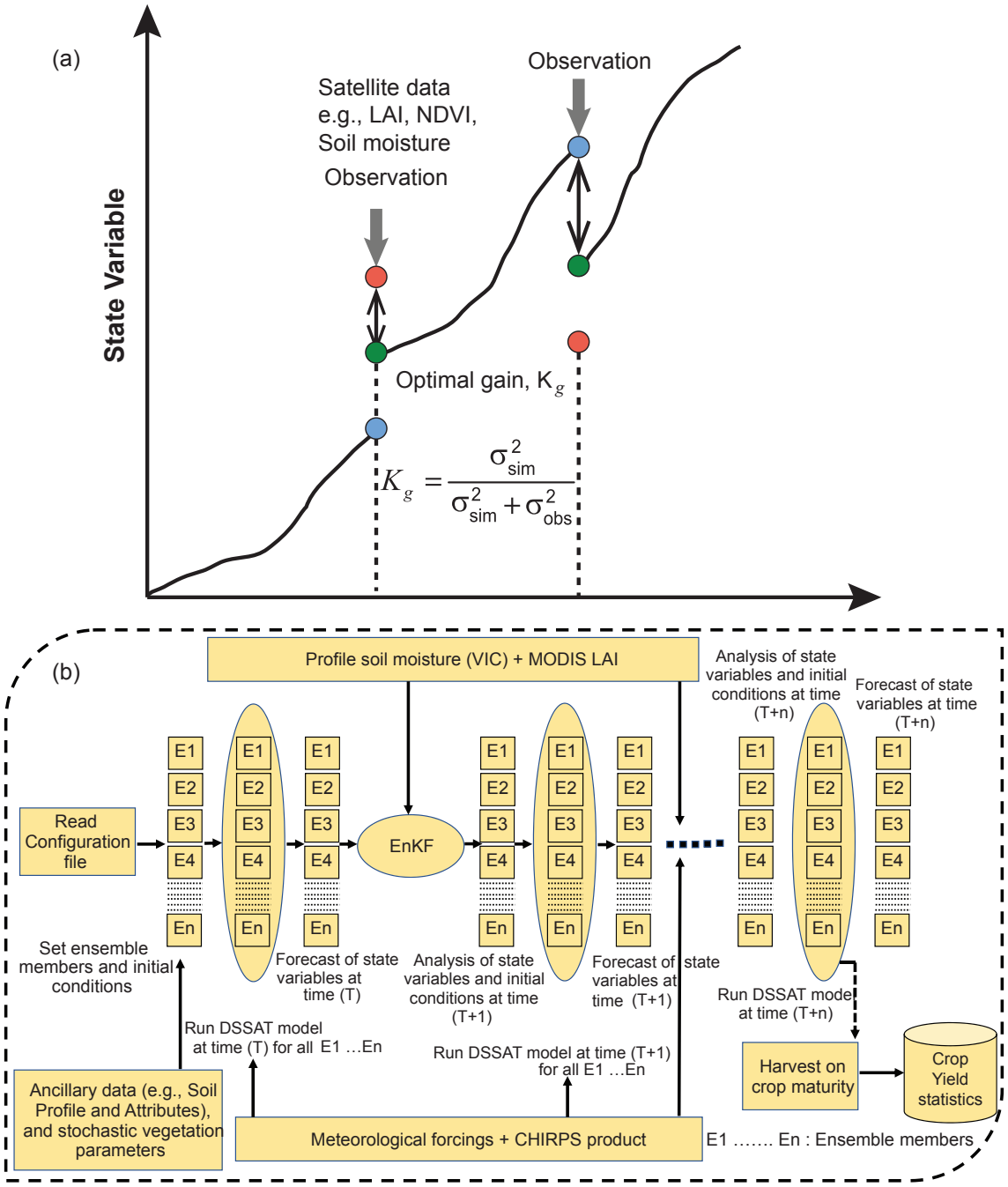

Fig. 3. Modified version of the crop model (*m*-DSSAT) using (a) the Ensemble Kalman Filter (EnKF). (b) VIC-generated soil moisture profiles and other vegetation related attributes (e.g., NDVI or LAI) are assimilated with the ensembles of *m*-DSSAT which can manage 50 ensemble members (represented by 'E').

3. Results and discussions

3.1. Model validation

As hydrological model outputs and state variables are heterogeneous in nature, it is challenging to validate them in data-poor regions over space and time. However, scientific validation with geophysical state variables provides an estimate of the skill of the model while addressing associated uncertainties. For the purpose of validating the RHEAS output, an independent source of data for a state variable is required. Soil moisture data from remote sensing is one such source. Another reason for using surface soil moisture has to do with the key nature of soil moisture as a variable that links the water and energy balances at the soil - atmosphere interface critical for many hydrologic processes. First, the VIC hydrologic model was validated against surface soil moisture over Cambodia. The NASA SMAP mission provides composite estimates of surface soil moisture for the top ~ 5 cm at a global extent. Taking advantage of such useful information on surface soil moisture conditions, we used the top layer soil moisture output from RHEAS to validate against the SMAP-based soil moisture in spatial and temporal fashion over Cambodia. The RHEAS model spatial resolution (25 km) is also nearly compatible with the SMAP observation spatial resolution of ~ 30 km. In general, the SMAP L-band radiometer does not observe soil moisture below ~ 5 cm depth. We also assume that the surface soil moisture dynamics is physically linked with the evolution of rootzone soil moisture. Hence, validating the surface moisture indirectly validates the rootzone soil moisture. The validation of annual mean soil moisture presented good accordance with observations (R^2 ~ 0.65) for the top 5

cm soil layer (Fig. 4a). The correlation between model outputs and observations consistently indicates a high correlation over most places, except some coastal areas and water bodies (e.g., Tonle Sap Lake), where the SMAP measurements are of inferior quality (Fig. 4b). As the SMAP soil moisture is an independent product, it is assumed to be suitable for validation against the VIC-generated profile surface soil moisture. In addition, validation with remote sensing observations also provides confidence in model performance. This is essential to ensure the accurate characterization of drought indices from the validated parameters. Hence, the results from the model can be used to define the agricultural/hydrologic drought status and the water stress conditions at various spatial–temporal scales.

Similarly, a regional scale validation was carried out using end-of-season yields, aggregated at country scale between 2000 and 2016. The interannual rice yields from *m*-DSSAT over Cambodia were validated against an independent source of yield records (obtained from FAO). Fig. 5 presents comparisons of observed and model-generated annual end-of-year yields. Soil and phenological data were collected for the period 2010–2013 and used in Wang et al. (2017) and the same genetic coefficients were used in our simulations as well; therefore, rice yield comparisons with data around this period are shown in Fig. 5 which exhibited good correlation ($R^2 \sim 0.84$) with very low bias between observed and RHEAS simulated yield estimates. However, extending the simulations to an earlier timeframe (2000–2008, Fig. S1) showed substantial bias compared to the latter part of the simulation period (2008–2016, Fig. 5). The large bias (~750 kg/ha) in the rice yields observed for the initial 5 years, i.e., 2000–2004 can be attributed to the following: (a) lack of farm management data, such as fertilizer application rates, and (b) subpar rice cultivar genetic coefficients. Although the calibrated cultivar genetic coefficients from Wang et al., 2017 were used throughout the simulation period, the lack of information on cultivar verities used during the initial period is a source of significant uncertainty. We anticipate that a change in rice cultivars might be one of the reasons for such disparate behavior of yields. Incorporating a calibrated cultivar variety for years 2000–2004 could potentially improve the rice yields; however, such calibration would call for additional data that are not available.

Accurate estimation of these variables is heavily reliant on the input data quality (e.g., meteorological forcing, vegetation), and large uncertainties can be expected due to the lack of detailed information on cultivar type, planting dates, etc. as well physical inaccessibility of some sites (e.g., station-based measurements) which hinder efforts to quantify the agricultural states. However, field data during the initial period of simulation (2000–2004) under no stress condition are not available. Another reason for such disparate behavior is probably due to the application of low fertilizer rates (5 kg/ha) based on data from FAO/World Bank for this period. This low fertilizer application rate is probably a major contributor to the large bias during the initial years of study; however, we have no other means in Cambodia to verify the FAO fertilizer application rates during the initial years. In the recent past, the farm management data collection through various agencies working in Cambodia has improved and that reflects in the much better results from year 2005 onwards.

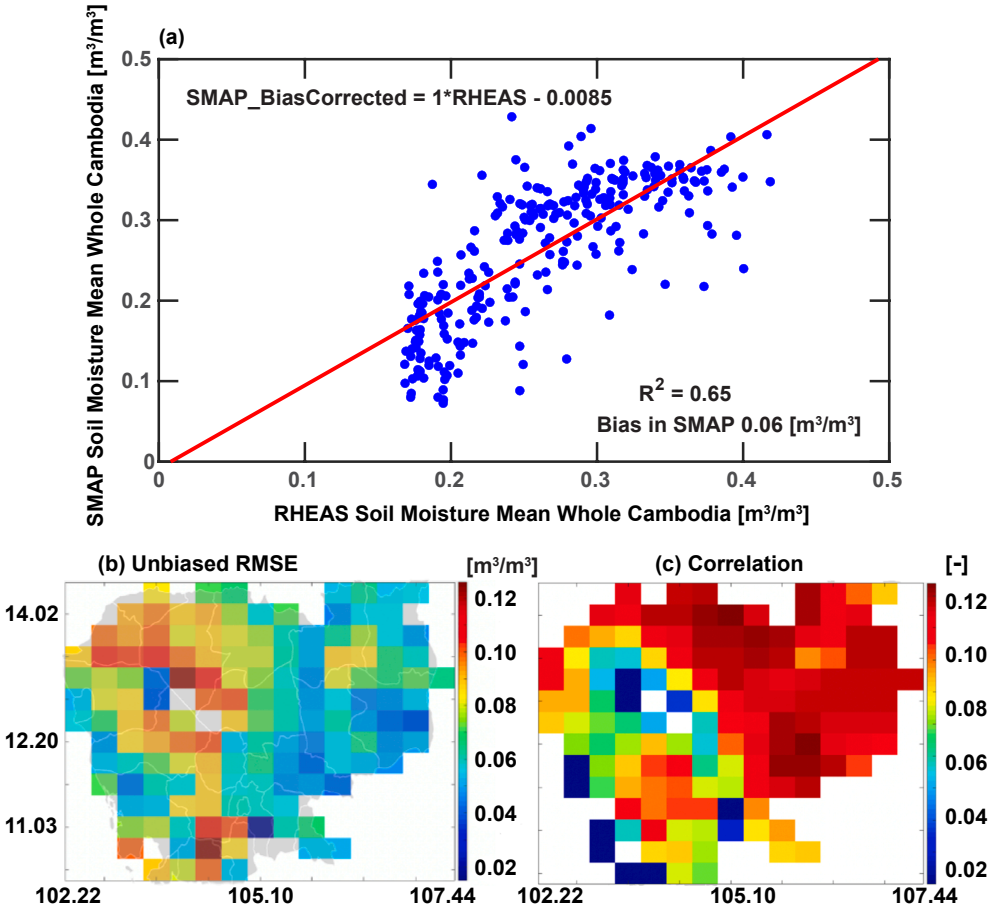

Fig. 4. (a, top panel) RHEAS-generated surface soil moisture compared with SMAP soil moisture in 2017 over Cambodia (b, bottom panel) Unbiased RMSE and (c, bottom panel) Correlation for RHEAS-based surface soil moisture for 2016 and 2017 data when compared with the SMAP surface soil moisture data (L3_SM_P) at 36 km EASE2 grid resolution.

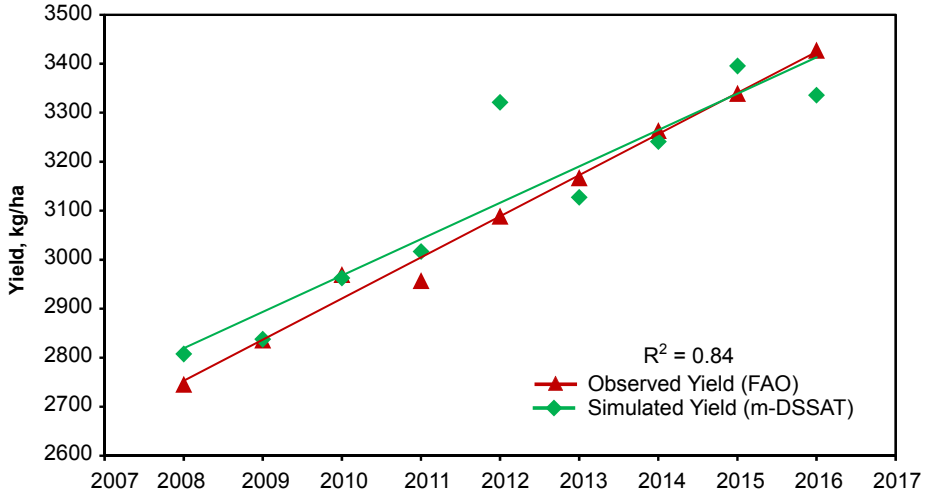

Fig. 5. Comparison of RHEAS (*m*-DSSAT)-simulated rice yields with actual observations (FAO) over Cambodia between 2008 and 2016.

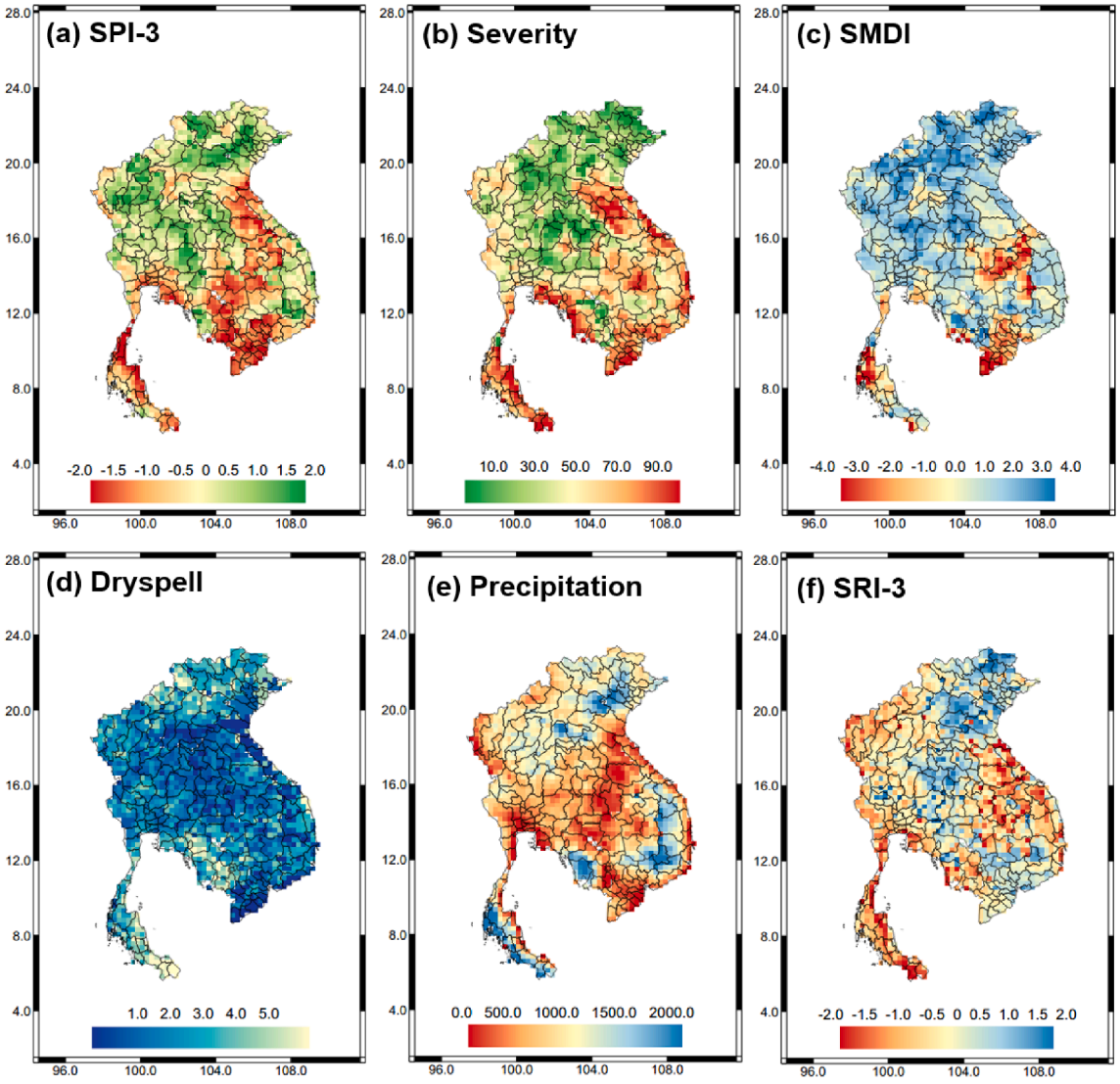

Fig. 6. Spatial distribution of RHEAS drought products over LMB: (a) 3-month Standardized Precipitation Index (SPI3) for March-April-May (MAM) (b) Agricultural drought severity for MAM (c) Soil Moisture Deficit Index values (SMDI) during the last week of May (d) Dry spells for the MAM period (e) Precipitation totals (in mm) for MAM (f) 3-month Standardized Runoff Index (SRI3) for MAM.

3.2. Hydrological modeling

Based on the final products (e.g., soil moisture profile, runoff, evapotranspiration) derived from the VIC hydrologic model, common drought monitoring indices were produced over the LMB region. Fig. 6. illustrates the sample outputs based on RHEAS drought indicators for 2014. Both rows present the fundamental drought indicators, including the 3-month standardized precipitation index, agricultural drought severity, and soil moisture deficit, dry spells, and standardized runoff index. As seen, the Mekong plain, comprising of low-lying areas of Cambodia, Lao PDR, and the Mekong delta, had been under severe stress throughout the year. Based on the probability of seasonal precipitation, the aggregated 3-month SPI reflects the short-term moisture conditions while the drought severity provides a standardized measurement (i.e., fluctuations/anomalies) of the moisture deficit (dry/wet) at the root zone. It should be noted the 3-month standardized precipitation index (and other indices) may be exhibiting a slightly lower value due to the spatial averaging, whereas in reality some grids may have values as low as −3. The soil moisture deficit index apprises the potential crop water extraction amount from different soil depths during various stages of crop growth. It takes the spatial average of a particular week of every month into account instead of averaging it temporally over the entire month. The northern parts of the LMB show SMDI value of + 3, representing higher root zone moisture availability. The bottom row shows the overall dry spells, annual precipitation totals, and the standardized runoff index. It should also be noted, the large spatial variability in all the drought indicators reflects the large spatial distribution of wet/dry conditions across the region. As most of the drought indices are based on the core hydrologic variables (such as precipitation and soil moisture), the indices follow a similar pattern. This behavior is quite evident, wherein the areas under stress remain congruent for all the indices irrespective of their nature of quantification (e.g., 'precipitation' for 'SPI', and 'soil moisture' for 'SMDI/Severity'). For the snapshots shown in Fig. 6., RHEAS showcased reasonable performance in capturing the drought stress. As shown, all the indicators exhibited a consistent stress in the drought-striven regions. The 3-month SPI, precipitation, and SRI3 indicators exhibited consistent spatial stress over Cambodia, southern Lao, lower stretches of Thailand and the Vietnam delta. Similarly, the soil moisture deficit index and drought severity depicted a similar behavior over the same regions. To gain in-depth knowledge of the persistence/behavior of drought in the region, a detailed study was carried out over Cambodia.

Fig. S2 (Supplementary Material) illustrates the differences in the behavior of SPI and SRI indices over Cambodia at various timescales for the years 1990–2019. As SPI and SRI are based on the standard deviations of precipitation and runoff from median values for long-term period, they were used to evaluate the relationship between precipitation conditions and hydrological conditions and characterizing the nature of drought on a range of timescales. The analysis indicated the exposure of the region to extreme dry/wet conditions over a period of 30 years. The 3-month SPI (SPI3) exhibited a frequent change in dry/wet conditions than the longer duration equivalent (i.e., SPI6 and SPI12). The SPI3 (and SPI1) was more effective in capturing the precipitation trends (and short- and medium-term moisture availability) during the rice-growing season. The SPI3 and SRI3 better captured the seasonal anomalies (proportion of dry or wet months) within a year, notably during the 1988–99 and 2015–16 drought events (Guo et al., 2017). However, these shorter timescale indices (SPI1/SRI1 or SPI3/SRI3) can be misleading in regions with normal to mild wetness (or normal dryness) for a particular 3-month period. This interpretation emerges due to potentially inaccurate accumulation of impacts on shorter time scales, wherein the wetness (or dryness) for that 3-month period depicts a temporary wet (dry) period. Hence, the larger timescale meteorological indices (SPI6/SRI6 or SPI12/SRI12) are much more effective in quantifying long-term wet or dry season trends. The SPI and SRI exhibit a similar pattern at larger timescales (12-month). The 3-month SPI and SRI behave distinctly wherein the SRI tends to be less variable than SPI due to the storage of incoming precipitation as soil moisture that limits the amount of surface runoff. This behavior can be clearly seen during the drought events of 1998–99 and 2015–16, where the 3-month SPI and SRI follow a slightly different pattern with a lag as compared to the respective 12-month timeframe. As the 12-month indices are based on the cumulative result of shorter periods, SPI and SRI show a lower frequency of positive and negative standardized values when compared to the 3-month values. Fig. S3 (Supplementary Material) shows the mean annual precipitation and runoff over Cambodia for the years 1990–2019. There was a clear indication of seasonal influence in the region, with prevailing wet periods at the start of the growing season (June onwards), and subsequent dry conditions from Nov-Mar.

Furthermore, a detailed regional study was carried out for the 2015 drought year, illustrated in Fig. 7. The spatial variability in drought severity (intensity) for Mar-Apr-May (MAM) and Jun-Jul-Aug (JJA) was well captured by RHEAS, exhibiting higher stress during the initial time period compared to the latter (Fig. 7a). Similarly, the spatial distribution of the soil moisture deficit index shows good agreement with drought severity (Fig. 7c). A comparison of the moisture deficit between the 22nd week (4th week of May) and 33rd week (2nd week of Aug) clearly shows a higher moisture deficit during the initial period of the year. Though the overall annual precipitation totals have increased over the years (except for the drought years), the interannual spatial variability shows lower levels of rainfall during MAM as compared to JAS (Fig. 7d). The 3-month SPI during the initial months (FMA) exhibited a relative moderate to severe dry conditions over the region while the latter period (JJA) presented a near normal to moderate wet conditions due to the onset of the southwest monsoon (Fig. 7b). The SPI3 index provides a better estimation of precipitation deficit and short-to-medium term moisture conditions and is considered critical in capturing the precipitation trends during reproductive and early grain-filling stages. Similarly, dry spells are used to detect significant changes in drought frequency due to the fluctuations in water/energy fluxes. Overall, there had been a consistent prevalence of high-stress conditions during the initial time period (April onwards) as compared to the mid-months, with extreme stress conditions in the southeast provinces of Prey Veng and Takeo, and normal to moderate dry conditions over the western provinces of Pailin and Battambang.

3.3. Crop modeling

The other objective of this study was the estimation of interannual rice yields over Cambodia, so that growers and policymakers could reduce agricultural losses due to drought events. Fig. S4a-c (Supplementary Material) presents the annual yields over Cambodia in 2005 and 2015, simulated from the *m*-DSSAT crop model within the RHEAS framework. There is a clear indication of an increase in yields (2900 kg/ha in 2005 to 3550 kg/ha in 2015) over the years; however, the drought-striven provinces exhibited identical patterns of low yields over the 10-year period, mostly due to the frequent exposure of prolonged periods of dry spells. However, the Tonle Sap basin and nearby areas have seen an increase in rice yields over the 10-yr period, partly due to the improvement in technology and farm management practices. Fig. S4d (Supplementary Material) presents the average yields over each province for the entire study period (2000–2016), clearly indicating low yields in the southeast regions. The low yield over the southeast provinces can also be well-matched with the drought indicators from the VIC model, wherein the provinces with high precipitation deficit and severity experienced lower productivity. However, the western provinces (e.g., Battambang) exhibit higher yields despite high exposure to drought events. The reason for such behavior can be attributed to the differences in soil properties and the better adaptability of paddy to local conditions. Nonetheless, specific improvements and analysis are being currently carried out on a regional basis to further improve the performance and stability of the RHEAS framework. In addition, the next

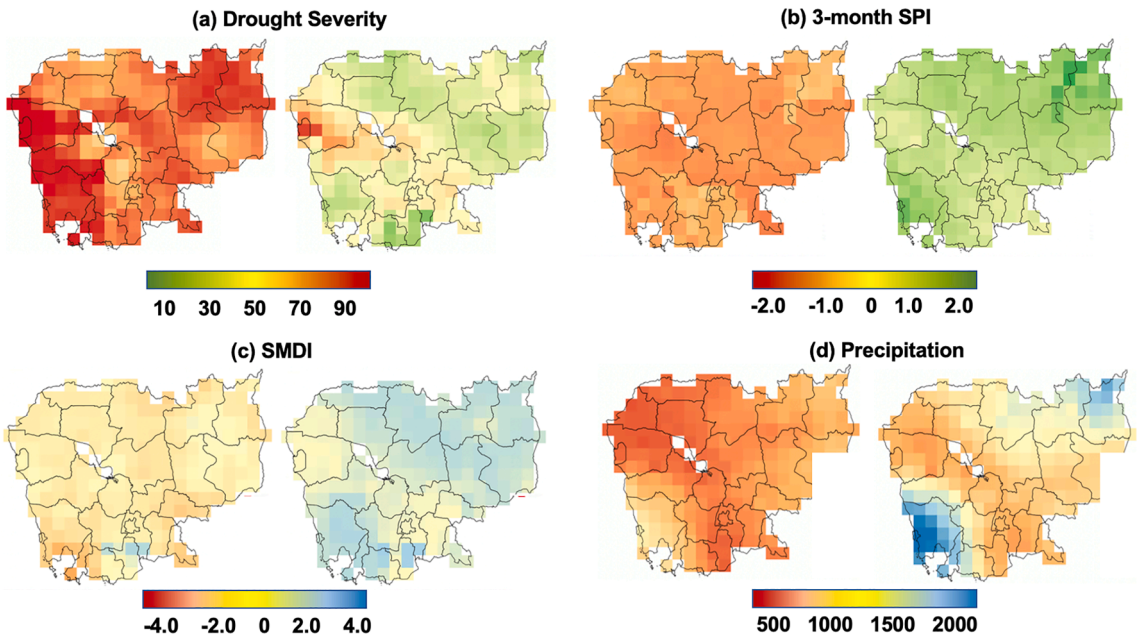

Fig. 7. Drought data products: Maps of a) Agricultural Drought Severity for MAM and JJA b) 3-month Standardized Precipitation Index (SPI3) during FMA and JJA c) Soil Moisture Deficit Index during 22nd and 33rd week d) Precipitation totals during MAM and JAS, showing the interannual variability for the 2015 drought year over Cambodia.

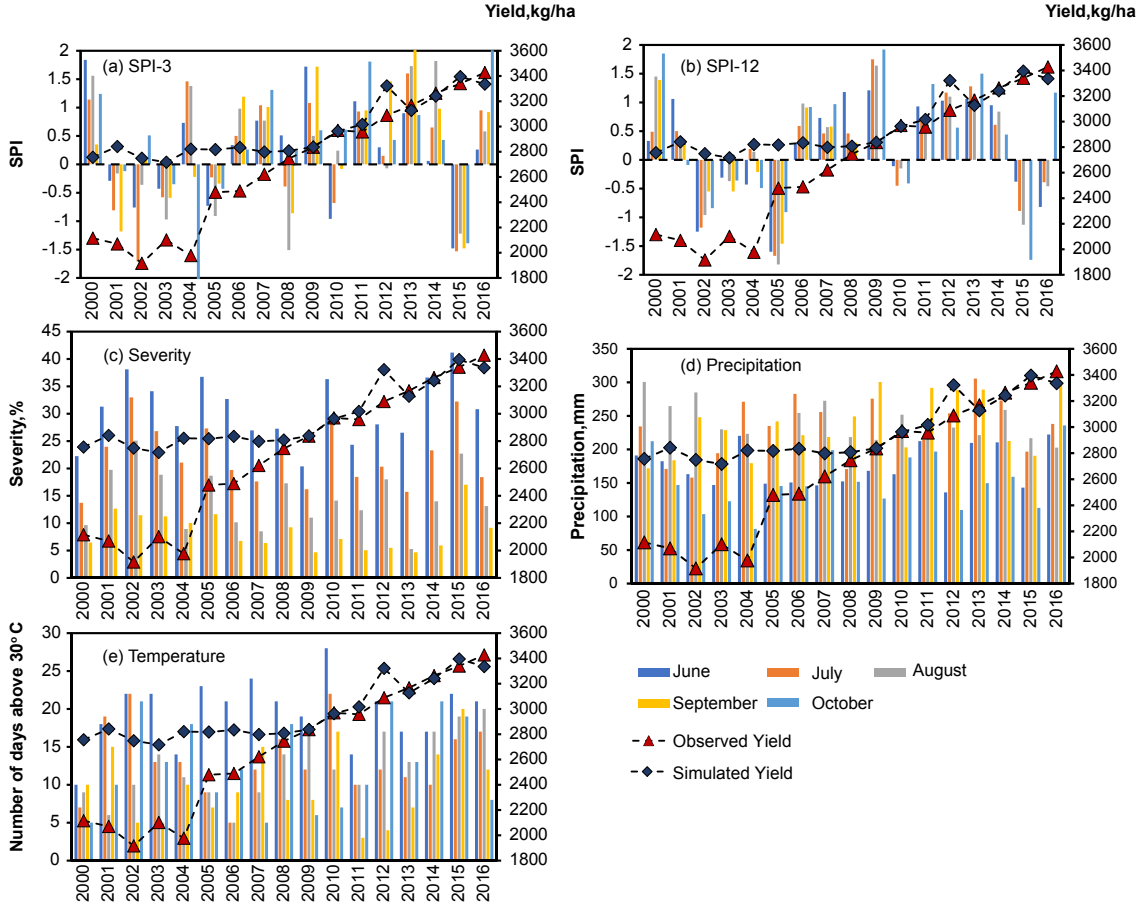

Fig. 8. Comparison of yield responses to: (a) growing season 3-month SPI (b) 12-month SPI (c) agricultural drought severity (d) precipitation totals (e) number of days above 30 °C for the growing season (Jun-Oct) from 2000 to 2016.

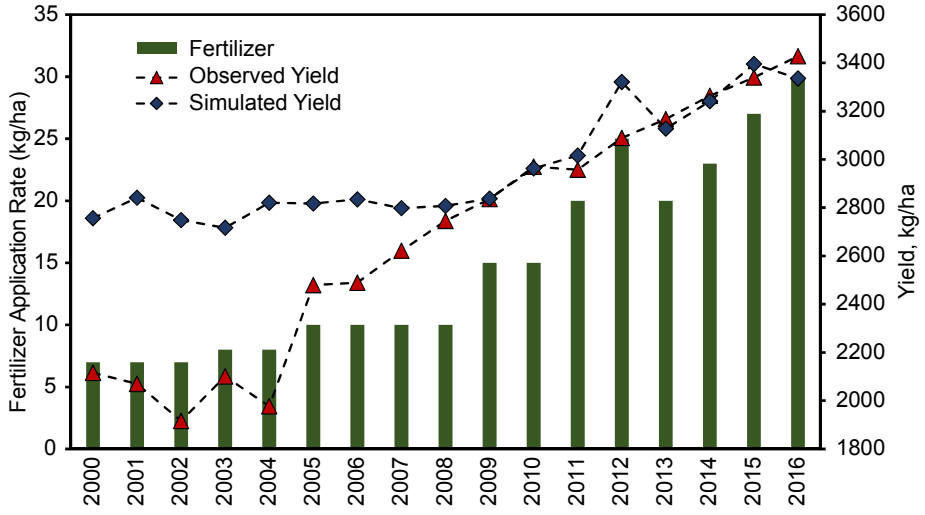

Fig. 9. Fertilizer application rates for the study period (2000–2016) compared with annual rice yields over Cambodia.

phase of studies would include assimilation of various state variables (e.g., NDVI) which would further improve model performance.

3.4. Correlation with crop yield

Fig. 8 presents a comparison of the impact of growing season (JJASO) rice yields with the standardized drought indices and hydrologic variables over Cambodia between 2000 and 2016. We evaluated the drought severity, precipitation totals, number of days exceeding temperatures of 30 °C, etc., for the growing season against observed and simulated yields. While simulations based on crop models anticipate water supply substantially driving crop yields, capturing the relationship between weather and crop yields shows no clear association. As shown in Fig. 8, the climatology of the drought indices predominantly remains the same, having negligible impact on annual rice yields. This can be better represented during the drought year 2015, wherein the annual yields increased despite the prevalence of stress conditions throughout the country. However, this situation can be better interpreted by the decrease in yield in 2016, mainly due to the persistence of drought spell from 2015 until mid-2016. Overall, we see a continuous increase in annual yields irrespective of the stress conditions, and no conclusive pattern in the behavior of drought parameters and crop yields can be deduced on a regional basis. As drought is primarily a local phenomenon, such trends may be more distinct on provincial levels (Fig. S4, Supplementary Material). Simulated yields are shown for selected provinces (e.g., Pailin, Preah Vihear), but due to the lack of actual provincial yields data, conclusions could not be drawn from the analysis. The severity index and precipitation totals showed a good correlation, with the prevalence of severe stress conditions (i.e., high severity and lower precipitation) during the start of growing season (June), and a gradual reduction of stress conditions (i.e., less severity and increased precipitation) in the subsequent months (Sep-Oct). Similarly, we investigated the number of days with air temperature exceeding 30 °C (Fig. 8e) within each growing season to identify any noticeable impact on agricultural yields. Most crops have an energy budget from sowing to harvest, accounted for using the Growing-Degree-Day (GDD) which was computed based on the maximum, minimum, and average ambient temperatures. However, the plant productivity (photosynthetic capacity) almost becomes negligible above an average temperature of 30 °C. Therefore, we analyzed the number of days where the ambient average temperature is above 30 °C to evaluate the stress on the crop. We found record number of days above 30 °C in the planting season during the stress periods, most notably during the 2015–2016 drought event. Likewise, the standardized drought indices (3, 12-month SPI), drought severity, and precipitation totals were examined.

The 3- and 12-month SPI for the growing season period (Jun-Oct) were compared with the rice yields to analyze the stress conditions during the growing season (Fig. 8a and 8b). The 3-month index was used to capture the short- and medium-term moisture conditions and estimate the precipitation trends during the important stages of crop growth, whereas the 12-month standardized index provided a cumulative overview of the short-term precipitation patterns (i.e., long-term precipitation patterns). RHEAS was able to capture the decrease in yield during the drought events of 2002, 2004 and 2008 but exhibited a contrasting behavior during the later drought events (e.g., 2010, 2015). It should be noted that the agreement between the drought indices and yield only accounts for the physical changes within the growing season. However, the growing season drought variability invariably remains normal to mild wet (SPI > 0) for most years (2005 onwards) during the simulation period, thus following an increasing trend of rice yields during those years.

As shown in Fig. 8, the growing season (Jun-Oct) exhibited negligible impact from water stress conditions. However, the study does not categorically indicate the prevalence of stress-free conditions throughout the study period. Instead, as shown in Fig. 7, stress conditions mostly occurred during the initial months (Feb-May) which subsequently alleviated to mild/near-normal conditions at the onset of the growing season. As the drought conditions were notably significant in capturing the interannual yield variability, we evaluated other management factors (such as fertilizer application rates, cultivar varieties) that could possibly drive the associated changes. Since the meteorological variables (e.g., precipitation, ambient temperature, etc.) and cultivar varieties (from Wang et al., 2017) remained same throughout the study period, the only variable factor in the analysis was the rate of fertilizer application (adopted from FAO/World Bank).

Since 2008, the fertilizer rates have steadily increased over the years, echoing a strong resemblance with observed and simulated yields (Fig. 9). A strong correlation is noted between observed yields and fertilizer application rates during the 2008–2016 period ($R^2 \sim 0.84$) with a similarly high value between simulated yields and fertilizer rates ($R^2 \sim 0.92$). Although less information was available on the local application rates, a significant pattern can be noted from the analysis. With increased consumption of fertilizer rates since 2008, the interannual yields have been steadily increasing each year as seen in Fig. 9. Prior to the aforementioned period, the fertilizer application rates remained the same, hence the initial timeframe (2000–2005) arrayed lower yields. As the management practices (e.g., fertilizer application rates) in a country

depend on the socioeconomic conditions of the farmers and the support of local governments, the fertilizer application rates in Cambodia have still not reached optimum levels (compared to the neighboring Mekong countries such as Vietnam and Thailand) and exhibit abundant scope for improvement in the near future. Hence, considering the results obtained from RHEAS, the consistent increase in yield can be significantly attributed to the application of chemical-based fertilizers.

4. Conclusions

The RHEAS framework facilitates end-to-end modeling that helps understand the impacts of evolving weather, hydrology, climate, and farm management practices on the crop status and yield, thus making its design unique. Based on the current application, RHEAS showed reasonable performance in capturing the agricultural and meteorological drought variability over LMB based on the information available from the drought indices. The results from the study depicted a common persistence of mild-medium dry conditions over Cambodia during the initial months, but the overall stress dwindles with the onset of monsoon at the start of the growing season (June onwards). In short, the Feb-May period witnesses significant stress conditions, whereas the growing season (post-June) achieved a near-normal to moderate wet conditions. Although, mean annual precipitation has seen an increase over the years, barring a few drought years, there has been a decrease in dry season precipitation due to the irregularities in weather regimes. However, the continuous prevalence of severe drought events, notably in 2015–16, has raised fears of occurrence of similar stress conditions in the drought-prone provinces.

Considering the results obtained from RHEAS, there is a clear indication of a significant increase of drought prevalence in most areas of the LMB, that may or may not have serious implications on the agriculture sector. The rice yields in Cambodia have been steadily witnessing an upward trend since the last decade, mainly due to increasing fertilizer application rates, and to some extent, due to the modernization of farm practices/techniques, mechanization and improvements in technology. The Mekong River Commission has cited a similar conclusion in their annual reports (MRC, 2014) of an increase in annual production of the four major crops (including rice). RHEAS was able to adequately capture the interannual variability of rice yields with observations ($R^2 \sim 0.84$) with low bias from 2005 onwards. The growing season hydrologic stress conditions when compared with annual yields also did not reflect any significant effect on the crop status barring a few drought years. However, the drought indices exhibited lower agricultural yields in the water-stress provinces (located in the Southeast regions) of Cambodia throughout the study period, thus reflecting the impact of drought on crop status at provincial levels. While the aforementioned situation envisages lower future yields due to elevating stress conditions, substantial arguments can be made on comparing drought conditions with annual yields. Drought solely does not affect agricultural yields as Cambodia inherently gets affected by flash flooding/waterlogging, possibly resulting in decreased yields and crop losses. As the meteorological variables and cultivar type were kept the same throughout the study period, the only variable factor for attaining higher yields can be attributed to the use of chemical fertilizers. Although the fertilizer application rates in Cambodia are well behind the neighboring Mekong countries (Vietnam and Thailand), there is much scope for improvement in the future.

CRediT authorship contribution statement

Abhijeet Abhishek: Formal analysis, Investigation, Writing - original draft. **Narendra N. Das:** Conceptualization, Methodology, Funding acquisition, Investigation, Project administration, Software, Writing - review & editing, Supervision. **Amor V.M. Ines:** Methodology, Investigation, Writing - review & editing, Supervision. **Konstantinos M. Andreadis:** Conceptualization, Software, Investigation, Writing - review & editing. **Susantha Jayasinghe:** Resources, Data curation, Writing - review & editing. **Stephanie Granger:** Conceptualization, Writing - review & editing. **Walter L. Ellenburg:** Resources, Writing - review & editing. **Rishiraj Dutta:** Resources, Data curation, Writing - review & editing. **Nguyen Hanh Quyen:** Resources, Data curation, Writing - review & editing. **Amanda M. Markert:** Project administration, Resources, Writing - review & editing. **Vikalp Mishra:** Resources, Writing - review & editing. **Mantha S. Phanikumar:** Funding acquisition, Investigation, Methodology, Project administration, Resources, Writing - review & editing, Supervision.

Declaration of Competing Interest

The authors declare that they have no known competing financial interests or personal relationships that could have appeared to influence the work reported in this paper.

Acknowledgements

The work was supported by the NASA-U.S. Agency for International Development (USAID) SERVIR-Mekong joint project, housed at the Asian Disaster Preparedness Center (ADPC) in Bangkok, Thailand. We acknowledge the support of NASA ROSES Grant: 18-SERVIR18_2 funding for development of the RHEAS integrated framework. We thank the support from the SERVIR Coordination Office, especially Dr. Ashutosh Limaye, and the NASA Program Manager Dr. Nancy Searby for their guidance and facilitating the project collaboration with USAID.

Appendix A. Supplementary data

Supplementary data to this article can be found online at https://doi.org/10.1016/j.jhydrol.2021.126291.

References

Aadhar, S., Mishra, V., 2017. High-resolution near real-time drought monitoring in South Asia. Sci. Data 4, 170145. https://doi.org/10.1038/sdata.2017.145.

ADB, 2009. The Economics of Climate Change in Southeast Asia: A Regional Review. Asian Development Bank, Manila, Philippines.

Andreadis, K.M., Clark, E.A., Wood, A.W., Hamlet, A.F., Lettenmaier, D.P., 2005. Twentieth-Century Drought in the Conterminous United States. J. Hydrometeorol. 6, 985–1001. https://doi.org/10.1175/JHM450.1.

Andreadis, K.M., Das, N., Stampoulis, D., Ines, A., Fisher, J.B., Granger, S., Kawata, J., Han, E., Behrangi, A., 2017. The Regional Hydrologic Extremes Assessment System: a software framework for hydrologic modeling and data assimilation. PLoS One 12, e0176506. https://doi.org/10.1371/journal.pone.0176506.

Arrouays, D., Grundy, M.G., Hartemink, A.E., Hempel, J.W., Heuvelink, G.B.M., Hong, S. Y., Lagacherie, P., Lelyk, G., McBratney, A.B., McKenzie, N.J., Mendonca-Santos, M. d. L., Minasny, B., Montanarella, L., Odeh, I.O.A., Sanchez, P.A., Thompson, J.A., Zhang, G.-L., 2014. GlobalSoilMap, in: Advances in Agronomy. pp. 93–134. 10.1016/B978-0-12-800137-0.00003-0.

Beran, B., Piasecki, M., 2009. Engineering new paths to water data. Comput. Geosci. 35, 753–760. https://doi.org/10.1016/j.cageo.2008.02.017.

Boote, K.J., 1999. Concepts for calibrating crop growth models. In: Hoogenboom, G., Wilkens, P.W., Tsuji, G.Y. (Eds.), DSSAT version 3, Vol. 4. University of Hawaii, Honolulu, pp. 179–199.

Dai, A., 2013. Increasing drought under global warming in observations and models. Nat. Clim. Chang. 3, 52–58. https://doi.org/10.1038/nclimate1633.

Das, N.N., Mohanty, B.P., 2006. Root Zone Soil Moisture Assessment Using Remote Sensing and Vadose Zone Modeling. Vadose Zo. J. 5, 296–307. https://doi.org/10.2136/vzj2005.0033.

Das, N.N., Mohanty, B.P., Cosh, M.H., Jackson, T.J., 2008. Modeling and assimilation of root zone soil moisture using remote sensing observations in Walnut Gulch Watershed during SMEX04. Remote Sens. Environ. 112, 415–429. https://doi.org/10.1016/j.rse.2006.10.027.

Duffy, P.B., Brando, P., Asner, G.P., Field, C.B., 2015. Projections of future meteorological drought and wet periods in the Amazon. Proc. Natl. Acad. Sci. 112, 13172–13177. https://doi.org/10.1073/pnas.1421010112.

Evensen, G., 2003. The Ensemble Kalman Filter: theoretical formulation and practical implementation. Ocean Dyn. 53, 343–367. https://doi.org/10.1007/s10236-003-0036-9.

Friedl, M.A., Sulla-Menashe, D., Tan, B., Schneider, A., Ramankutty, N., Sibley, A., Huang, X., 2010. MODIS Collection 5 global land cover: algorithm refinements and characterization of new datasets. Remote Sens. Environ. 114, 168–182. https://doi.org/10.1016/j.rse.2009.08.016.

Funk, C., Peterson, P., Landsfeld, M., Pedreros, D., Verdin, J., Shukla, S., Husak, G., Rowland, J., Harrison, L., Hoell, A., Michaelsen, J., 2015. The climate hazards infrared precipitation with stations—a new environmental record for monitoring extremes. Sci. Data 2, 150066. https://doi.org/10.1038/sdata.2015.66.

Gebremeskel Haile, G., Tang, Q., Sun, S., Huang, Z., Zhang, X., Liu, X., 2019. Droughts in East Africa: causes, impacts and resilience. Earth-Science Rev. 193, 146–161. https://doi.org/10.1016/j.earscirev.2019.04.015.

Godfray, H.C.J., Beddington, J.R., Crute, I.R., Haddad, L., Lawrence, D., Muir, J.F., Pretty, J., Robinson, S., Thomas, S.M., Toulmin, C., 2010. Food security: the challenge of feeding 9 billion people. Science (80-.) 327, 812–818. https://doi.org/10.1126/science.1185383.

Grillakis, M.G., 2019. Increase in severe and extreme soil moisture droughts for Europe under climate change. Sci. Total Environ. 660, 1245–1255. https://doi.org/10.1016/j.scitotenv.2019.01.001.

Guo, H., Bao, A., Liu, T., Ndayisaba, F., He, D., Kurban, A., De Maeyer, P., 2017. Meteorological Drought Analysis in the Lower Mekong Basin Using Satellite-Based Long-Term CHIRPS Product. Sustainability 9, 901. https://doi.org/10.3390/su9060901.

Han, E., Ines, A.V.M., Koo, J., 2019. Development of a 10-km resolution global soil profile dataset for crop modeling applications. Environ. Model. Softw. 119, 70–83. https://doi.org/10.1016/j.envsoft.2019.05.012.

Hao, C., Zhang, J., Yao, F., 2015. Combination of multi-sensor remote sensing data for drought monitoring over Southwest China. Int. J. Appl. Earth Obs. Geoinf. 35, 270–283. https://doi.org/10.1016/j.jag.2014.09.011.

Hoang, L.P., van Vliet, M.T.H., Kummu, M., Lauri, H., Koponen, J., Supit, I., Leemans, R., Kabat, P., Ludwig, F., 2019. The Mekong's future flows under multiple drivers: how climate change, hydropower developments and irrigation expansions drive hydrological changes. Sci. Total Environ. 649, 601–609. https://doi.org/10.1016/j.scitotenv.2018.08.160.

Houtekamer, P.L., Mitchell, H.L., 1998. Data assimilation using an ensemble Kalman filter technique. Mon. Wea. Rev. 126, 796–811 https://doi.org/10.1175/1520-0493(1998)126<0796:DAUAEK>2.0.CO;2.

Ines, A.V.M., Das, N.N., Hansen, J.W., Njoku, E.G., 2013. Assimilation of remotely sensed soil moisture and vegetation with a crop simulation model for maize yield prediction. Remote Sens. Environ. 138, 149–164. https://doi.org/10.1016/j.rse.2013.07.018.

IPCC, 2007. Climate change 2001. Weather. https://doi.org/10.1256/wea.58.04.

Johnston, R.., Hoanh, C.T.., Lacombe, G.., Lefroy, R.., Pavelic, P.., Fry, C., 2012. Managing water in rainfed agriculture in the Greater Mekong Subregion. 10.5337/2012.201.

Jones, J., Hoogenboom, G., Porter, C., Boote, K., Batchelor, W., Hunt, L., Wilkens, P., Singh, U., Gijsman, A., Ritchie, J., 2003. The DSSAT cropping system model. Eur. J. Agron. 18, 235–265. https://doi.org/10.1016/S1161-0301(02)00107-7.

Kalnay, E., Kanamitsu, M., Kistler, M., Collins, W., Deaven, D., Gandin, L., Iredell, M., Jenne, R., Joseph, D., 1996. The NCEP NCAR 40-year reanalysis project. Bull. Am. Meteorol. Soc.

Katsanos, D., Retalis, A., Michaelides, S., 2016. Validation of a high-resolution precipitation database (CHIRPS) over Cyprus for a 30-year period. Atmos. Res. 169, 459–464. https://doi.org/10.1016/j.atmosres.2015.05.015.

Kim, S., Shao, W., Kam, J., 2019. Spatiotemporal patterns of US drought awareness. Palgrave Commun. 5, 107. https://doi.org/10.1057/s41599-019-0317-7.

Kite, G., 2001. Modelling the Mekong: hydrological simulation for environmental impact studies. J. Hydrol. 253, 1–13. https://doi.org/10.1016/S0022-1694(01)00396-1.

Klisch, A., Atzberger, C., 2016. Operational drought monitoring in Kenya using MODIS NDVI time series. Remote Sens. 8, 267. https://doi.org/10.3390/rs8040267.

Lauri, H., Räsänen, T.A., Kummu, M., 2014. Using reanalysis and remotely sensed temperature and precipitation data for hydrological modeling in monsoon climate: Mekong River case study. J. Hydrometeorol. 15, 1532–1545. https://doi.org/10.1175/JHM-D-13-084.1.

Liang, X., Lettenmaier, D.P., Wood, E.F., Burges, S.J., 1994. A simple hydrologically based model of land surface water and energy fluxes for general circulation models. J. Geophys. Res. 99, 14415. https://doi.org/10.1029/94JD00483.

Liu, S., Lu, P., Liu, D., Jin, P., 2007. Pinpointing source of Mekong and measuring its length through analysis of satellite imagery and field investigations. Geo-spatial Inf. Sci. 10, 51–56. https://doi.org/10.1007/s11806-007-0011-6.

Mainuddin, M., Kirby, M., Hoanh, C.T., 2013. Impact of climate change on rainfed rice and options for adaptation in the lower Mekong Basin. Nat. Hazards 66, 905–938. https://doi.org/10.1007/s11069-012-0526-5.

Mishra, A.K., Singh, V.P., 2010. A review of drought concepts. J. Hydrol. 391, 202–216. https://doi.org/10.1016/j.jhydrol.2010.07.012.

Mizukami, N., P. Clark, M., G. Slater, A., D. Brekke, L., M. Elsner, M., R. Arnold, J., Gangopadhyay, S., 2014. Hydrologic Implications of Different Large-Scale Meteorological Model Forcing Datasets in Mountainous Regions. J. Hydrometeorol. 15, 474–488. 10.1175/JHM-D-13-036.1.

MRC, 2014. Crop production for food security and rural poverty Baseline and pilot modelling.

MRC, 2003. State of the Basin Report, State of the Basin Report Executive Summary. Phnom Penh, Cambodia.

Pandey, S., Bhandari, H., Ding, S., Prapertchob, P., Sharan, R., Naik, D., Taunk, S.K., Sastri, A., 2007. Coping with drought in rice farming in Asia: insights from a cross-country comparative study. Agric. Econ. 37, 213–224. https://doi.org/10.1111/j.1574-0862.2007.00246.x.

Pokhrel, Y., Shin, S., Lin, Z., Yamazaki, D., Qi, J., 2018. Potential disruption of flood dynamics in the lower Mekong River Basin due to upstream flow regulation. Sci. Rep. 8, 17767. https://doi.org/10.1038/s41598-018-35823-4.

Pozzi, W., Sheffield, J., Stefanski, R., Cripe, D., Pulwarty, R., Vogt, J.V., Heim, R.R., Brewer, M.J., Svoboda, M., Westerhoff, R., van Dijk, A.I.J.M., Lloyd-Hughes, B., Pappenberger, F., Werner, M., Dutra, E., Wetterhall, F., Wagner, W., Schubert, S., Mo, K., Nicholson, M., Bettio, L., Nunez, L., van Beek, R., Bierkens, M., de Goncalves, L.G.G., de Mattos, J.G.Z., Lawford, R., 2013. Toward global drought early warning capability: expanding international cooperation for the development of a framework for monitoring and forecasting. Bull. Am. Meteorol. Soc. 94, 776–785. https://doi.org/10.1175/BAMS-D-11-00176.1.

Sheffield, J., Wood, E.F., 2007. Characteristics of global and regional drought, 1950–2000: analysis of soil moisture data from off-line simulation of the terrestrial hydrologic cycle. J. Geophys. Res. 112, D17115. https://doi.org/10.1029/2006JD008288.

Sheffield, J., Wood, E.F., Chaney, N., Guan, K., Sadri, S., Yuan, X., Olang, L., Amani, A., Ali, A., Demuth, S., Ogallo, L., 2014. A drought monitoring and forecasting system for sub-sahara african water resources and food security. Bull. Am. Meteorol. Soc. 95, 861–882. https://doi.org/10.1175/BAMS-D-12-00124.1.

Son, N.T., Chen, C.F., Chen, C.R., Chang, L.Y., Minh, V.Q., 2012. Monitoring agricultural drought in the Lower Mekong Basin using MODIS NDVI and land surface temperature data. Int. J. Appl. Earth Obs. Geoinf. 18, 417–427. https://doi.org/10.1016/j.jag.2012.03.014.

Svoboda, M., LeComte, D., Hayes, M., Heim, R., Gleason, K., Angel, J., et al., 2002. The drought monitor. Bull. Am. Meteorol. Soc. 83, 1181–1190. https://doi.org/10.1175/1520-0477-83.8.1181.

Thilakarathne, M., Sridhar, V., 2017. Characterization of future drought conditions in the Lower Mekong River Basin. Weather Clim. Extrem. 17, 47–58. https://doi.org/10.1016/j.wace.2017.07.004.

Toté, C., Patricio, D., Boogaard, H., van der Wijngaart, R., Tarnavsky, E., Funk, C., 2015. Evaluation of satellite rainfall estimates for drought and flood monitoring in Mozambique. Remote Sens. 7, 1758–1776. https://doi.org/10.3390/rs70201758.

Van Loon, A.F., Gleeson, T., Clark, J., Van Dijk, A.I.J.M., Stahl, K., Hannaford, J., Di Baldassarre, G., Teuling, A.J., Tallaksen, L.M., Uijlenhoet, R., Hannah, D.M., Sheffield, J., Svoboda, M., Verbeiren, B., Wagener, T., Rangecroft, S., Wanders, N., Van Lanen, H.A.J., 2016a. Drought in a human-modified world: reframing drought definitions, understanding and analysis approaches. Hydrol. Earth Syst. Sci. Discuss. 1–34 https://doi.org/10.5194/hess-2016-251.

Van Loon, A.F., Gleeson, T., Clark, J., Van Dijk, A.I.J.M., Stahl, K., Hannaford, J., Di Baldassarre, G., Teuling, A.J., Tallaksen, L.M., Uijlenhoet, R., Hannah, D.M., Sheffield, J., Svoboda, M., Verbeiren, B., Wagener, T., Rangecroft, S., Wanders, N., Van Lanen, H.A.J., 2016b. Drought in the anthropocene. Nat. Geosci. 9, 89–91. https://doi.org/10.1038/ngeo2646.

Wang, Q., Chun, J.A., Lee, W.-S., Sanai, L., Seng, V., 2017. Shifting planting dates and fertilizer application rates as climate change adaptation strategies for two rice cultivars in Cambodia. J. Clim. Chang. Res. 8, 187–199. https://doi.org/10.15531/ksccr.2017.8.3.187.

Whitaker, J.S., Hamill, T.M., 2002. Ensemble data assimilation without perturbed observations. Mon. Weather Rev. 130, 1913–1924. https://doi.org/10.1175/1520-0493(2002)130<1913:EDAWPO>2.0.CO;2.

Wilhite, D.A., 2000. Chapter1 Drought as a Natural Hazard, in: Drought: A Global Assessment. pp. 3–18.

Wongchuig Correa, S., de Paiva, R.C.D., Espinoza, J.C., Collischonn, W., 2017. Multi-decadal hydrological retrospective: case study of amazon floods and droughts. J. Hydrol. 549, 667–684. https://doi.org/10.1016/j.jhydrol.2017.04.019.

Zhang, A., Jia, G., 2013. Monitoring meteorological drought in semiarid regions using multi-sensor microwave remote sensing data. Remote Sens. Environ. 134, 12–23. https://doi.org/10.1016/j.rse.2013.02.023.

Zhang, J., Mu, Q., Huang, J., 2016. Assessing the remotely sensed Drought Severity Index for agricultural drought monitoring and impact analysis in North China. Ecol. Indic. 63, 296–309. https://doi.org/10.1016/j.ecolind.2015.11.062.

Zhang, L., Jiao, W., Zhang, H., Huang, C., Tong, Q., 2017. Studying drought phenomena in the Continental United States in 2011 and 2012 using various drought indices. Remote Sens. Environ. 190, 96–106. https://doi.org/10.1016/j.rse.2016.12.010.

Zhang, Y., Pan, M., Sheffield, J., Siemann, A.L., Fisher, C.K., Liang, M., Beck, H.E., Wanders, N., MacCracken, R.F., Houser, P.R., Zhou, T., Lettenmaier, D.P., Pinker, R.T., Bytheway, J., Kummerow, C.D., Wood, E.F., 2018. A Climate Data Record (CDR) for the global terrestrial water budget: 1984–2010. Hydrol. Earth Syst. Sci. 22, 241–263. https://doi.org/10.5194/hess-22-241-2018.